Orienting cylindrical microdomains in polystyrene--*b*-poly(ethylene-*co*-butylene)-*b*-polystyrene triblock copolymer/diluent sheet by application of temperature gradient*)

Ryo Yamanaka[1), Nobutaka Shimizu[2), Noriyuki Igarashi[2), Hideaki Takagi[2), Shinichi Sakurai[1), **)

Abstract: The cylinder-forming polystyrene-*b*-poly(ethylene-*co*-butylene)-*b*-polystyrene (SEBS) triblock copolymer with a volume fraction of polystyrene (PS) equal to 0.16 was investigated. The orientation of cylindrical microdomains in SEBS/diluent sheet by application of temperature gradient were studied using small-angle X-ray scattering (SAXS). Dioctyl phthalate (DOP) was used as a diluent, which selectively dissolves SEBS, being a good solvent for PS but a poor solvent for poly(ethylene-*co*-butylene) (PEB). Due to this selectivity, a lamellar morphology was found at lower temperature (T_{cold}) for specimens with SEBS/DOP ratio of 6/4 and 7/3. It was further revealed that the morphology changed to be cylindrical at higher temperature (T_{hot}). The order-order transition temperature (T_{OOT}) was found to be 100 °C for both compositions, although a coexistence of lamellae and cylinders in a much wider temperature range was observed for the composition with SEBS/DOP = 7/3 as compared to the composition with SEBS/DOP = 6/4. These results indicate that the diluent selectivity of solubility at lower temperatures is suppressed at higher temperatures. For the specimen with SEBS/DOP = 6/4 the order-disorder transition temperature (T_{ODT}) was found to be 152.0 °C. The cylindrical morphology was found near the cold wall of the sample holder, even though the lamellar phase should be stable because the cold temperature was below T_{OOT}. This result implies that the temperature gradient may destabilize the lamellar phase. The cylinders in the confined space under the temperature gradient are considered to accommodate well. Both of the spacing and the cylinder radius was found to be larger as the position of the specimen irradiated by the incident X-ray beam was closer to the cold sidewall of the temperature gradient sample cell.

Keywords: polystyrene-*b*-poly(ethylene-*co*-butylene)-*b*-polystyrene triblock copolymer, diluent, cylindrical microdomains, perpendicular orientation, temperature gradient, small-angle X-ray scattering.

Orientowanie cylindrycznych mikrodomen w kompozycjach trójblokowego kopolimeru polistyren-*b*-poli(etylen-*co*-butylen)-*b*-polistyren z rozcieńczalnikiem za pomocą gradientu temperatury

Streszczenie: Do badań użyto kopolimeru blokowego polistyren-*b*-poli(etylen-*co*-butylen)-*b*-polistyren (SEBS), w którym ułamek objętościowy polistyrenu (PS) wynosił 0,16. Metodą rozpraszania promieni rentgenowskich pod małymi kątami (SAXS) oceniano zmiany orientacji cylindrycznych mikrodomen w kompozycjach SEBS/rozcieńczalnik po zastosowaniu gradientu temperatury. Jako rozcieńczalnik stosowano ftalan dioktylu (DOP), który wykazuje selektywność rozpuszczania SEBS – dobra rozpuszczalność PS, a słaba poli(etylenu-*co*-butylenu) (PEB). Z powodu tej selektywności, w przypadku próbek o stosunku SEBS/DOP wynoszącym 6/4 i 7/3, w niższej temperaturze (T_{cold}) stwierdzono morfologię lamelarną. Stwierdzono też, że w wyższej temperaturze (T_{hot}) morfologia zmieniała się w cylindryczną. Temperatura przemiany porządek-porządek (T_{OOT}) w obu kompozycjach wynosiła 100 °C, chociaż współistnienie lameli i cylindrów w znacznie szerszym zakresie temperatury stwierdzono w przy-

[1) Kyoto Institute of Technology, Department of Biobased Materials Science, Matsugasaki, Sakyo-ku, Kyoto 606-8585, Japan.
[2) Institute of Materials Structure Science, Photon Factory, High Energy Accelerator Research Organization, Oho 1-1, Tsukuba, Ibaraki 305-0801, Japan.

padku kompozycji SEBS/DOP = 7/3 w porównaniu z kompozycją SEBS/DOP = 6/4. Wyniki te wskazują, że w wyższej temperaturze selektywność rozpuszczania jest stłumiona. Stwierdzono też, że w próbce SEBS/DOP = 6/4 temperatura przemiany porządek-nieporządek (T_{ODT}) wynosi 152,0 °C. W pobliżu zimnej ściany uchwytu próbki, której temperatura była niższa niż T_{ODT}, zaobserwowano morfologię cylindryczną, chociaż spodziewano się stabilnej fazy lamelarnej. Oznacza to, że gradient temperatury może destabilizować fazę lamelarną. Uważa się, że w ograniczonej przestrzeni w warunkach gradientu temperatury lepsze dopasowanie jest możliwe w przypadku cylindrów. W miarę obniżania temperatury zarówno rozstaw, jak i promienie cylindrów stają się większe.

Słowa kluczowe: kopolimer polistyren-*b*-poli(etylen-*co*-butylen)-*b*-polistyren, rozcieńczalnik, cylindryczne mikrodomeny, orientacja prostopadła, gradient temperatury, metoda rozpraszania promieni rentgenowskich pod małymi kątami.

Control of orientation of nanostructures in polymeric materials has been attracting interests from academic and technological viewpoints because of demands of producing functional materials having anisotropic properties. Applying temperature gradient is one of the most promising tactics for controlling orientation in polymer systems. Perpendicular orientation was achieved for cylindrical microdomains in block copolymer thin films by the application of temperature gradient [1, 2]. It was also reported that the crystalline lamellae were formed parallel to the applied temperature gradient for a crystalline polymer [3]. These examples of the experimental studies clearly indicate the significance and the superiority of the application of the temperature gradient.

When temperature gradient is imposed to liquid system, a convective flow is induced [4, 5]. It has been reported that convection can be a useful tool for polymer blends so nicely to reorganize morphology during phase separation and to create quite interesting dissipative structures [6]. As for unique control of orientation in block copolymer systems, success of the lamellar microdomains orientation was firstly reported and then the more interesting orientation of cylindrical microdomains perpendicular to the films and to the applied temperature gradient was recently reported. In the former case, the temperature gradient was imposed in such a way that the hot (T_{hot}) and cold (T_{cold}) temperatures were $T_{cold} < T_{ODT} < T_{hot}$, where T_{ODT} stands for the order-disorder transition temperature [7, 8]. On the other hand, some researchers [1, 2] reported the perpendicular orientation of cylinders when the temperature gradient was imposed for specimens even below T_{ODT}, namely $T_{cold} < T_{hot} < T_{ODT}$ (so-called cold zone annealing). This method was more promising because the temperature required for thermal annealing (application of the temperature gradient) was much lower and therefore denoted a milder condition. It is noted that these methods are categorized as "zone annealing", where a specimen is forced to move very slowly in the hot and cold zones with temperatures set at T_{hot} and T_{cold}, respectively. To be contrast, we will provide much more milder temperature condition and more speedy condition in this present paper for the perpendicular orientation of cylinders by the application of the temperature gradient to the block copolymer/diluent system.

Perpendicular orientation of cylinders [9–15] has been attracting researcher's interests because of their potential applications for producing film specimens bearing an anisotropic mechanical property, or a unique optical performance, for producing nano-templates with nanometer-scale holes [13], and so forth. For instance, in case of hard cylinders with a soft matrix phase, such a film specimen having the perpendicularly oriented cylinders is tough against the compression, while it is easy to deform when stretched uniaxially or biaxially. Furthermore, such a film may have an anisotropic optical performance owing to the form birefringence of cylindrical particles [16] such that the film exhibits birefringence when viewed from the side (or from an inclined direction) while there is no birefringence when viewed from the normal direction [10]. Thus, this film can be used as a protector film for a smartphone or for a laptop computer to prevent others from furtive glances.

As a trial of inducing the perpendicular orientation of cylinders in a different way than using the temperature gradient, recent notable developments include utilization of the spontaneous directional coalescence of spheres induced by thermal annealing [9–11] or solvent vapor annealing [13, 14], and utilizing ability of mesogenic groups to form liquid-crystals, which are chemically bonded to one of the block components as pendant groups [12, 15]. For this case, it is striking that the cylinders completely passed through the film specimen with thickness of about 300 nm [15]. On the other hand, in the case of the directional coalescence of spheres induced by thermal annealing or solvent vapor annealing, the technique can be widely applied to many general block copolymers not having specific chemical groups (such as the mesogenic groups). Furthermore, it is also possible to attain the perpendicular orientation of cylinders in comparably thick films [10], although the cylinders do not perfectly pass through the film specimen. Due to such versatility, the method utilizing the directional coalescence of spheres is preferable. However, this method is limited to block copolymers for which a minor block content is slightly larger (so as to stabilize the cylindrical phase) than the value at the border between cylindrical and spherical phases. This is because non-equilibrium morphology (sphere) is required to be formed

in advance, which eventually transforms into the thermodynamically stable morphology (cylinder) upon the thermal or solvent annealing. Such a trivial control of morphologies requires a narrow window of the minor block component content, which should be slightly larger than the value at the border. In this regard, the application of the temperature gradient is considered to apply more widely to the general block copolymers, free from the composition requirement (as far as it is in a region that the cylindrical morphology is stable). Thus, we examined the ability of this method (application of the temperature gradient) for the induction of the perpendicular orientation of cylinders.

EXPERIMENTAL PART

Materials

The sample used in this study was a polystyrene--*block*-poly(ethylene-*co*-butylene)-*block*-polystyrene (SEBS) triblock copolymer with number-average molecular weight $\overline{M}_n = 6.60 \cdot 10^4$ and dispersity $\overline{M}_w/\overline{M}_n = 1.03$ ($\overline{M}_w$ – weight-average molecular weight) [9–11]. The total volume fraction of polystyrene (PS) end-blocks was 0.16. Since the middle poly(ethylene-*co*-butylene) (PEB) block comprises ethylene and butylene moieties, the composition should be clarified, which is the ethylene/butylene ratio being equal to 59/41 (by volume). Therefore, the overall composition in the SEBS sample was [PS end-block]/[ethylene moiety in PEB]/[butylene moiety in PEB]/[PS end-block] being equal to 8/50/34/8. Dioctyl phthalate (DOP) was used as the diluent. Note that DOP has selectivity in solubility for the SEBS, *i.e.*, good solubility for PS while poor solubility for PEB. Two specimens were prepared with compositions of SEBS/DOP ratio being 6/4 and 7/3.

Methods of testing

To impose temperature gradient to a specimen, we fabricated such a set up as schematically shown in Fig. 1.

The specimen was filled in the 3 mm gap space (36 mm x 3 mm) in an aluminum plate with thickness of 1 mm, as shown in Fig. 1a. Note here that notches were introduced in the sample cell at the both edges near the gap space so as to minimize heat flow from the hot to cold sides. Thus, the notch is the key to keep thermal insulation between the hot and cold sides. After the specimen was filled, the top and bottom of the specimen were covered with the polyimide film (25 µm thickness; Du Pont TORAY Co, Ltd., Japan) and cover slip (0.12–0.17 mm thickness; Matsunami Glass Ind., Ltd., Japan), respectively. The reason of using the polyimide film is to minimize the absorption of X-ray due to such window materials when conducting measurements of the two-dimensional small-angle X-ray scattering (2D-SAXS) for the nanostructure analyses, noting that the polyimide film is thinner than the cover slip so that the absorption is lesser. The sample cell filled with the specimen was then fabricated as shown schematically in Fig. 1b to impose the temperature gradient, where the right and left sides of the sample cell were sandwiched by the metal blocks of which temperatures were relatively lower and higher, respectively. The high temperature block was maintained by the electric heater, while the cold temperature by the water circulation supplied from a reservoir. Thermosensors which were the adhesive type chromel-alumel thermocouple (ST-50, RKC Instrument, Inc., Tokyo, Japan) were attached on the surface of the sample cell at the positions very close to the specimen
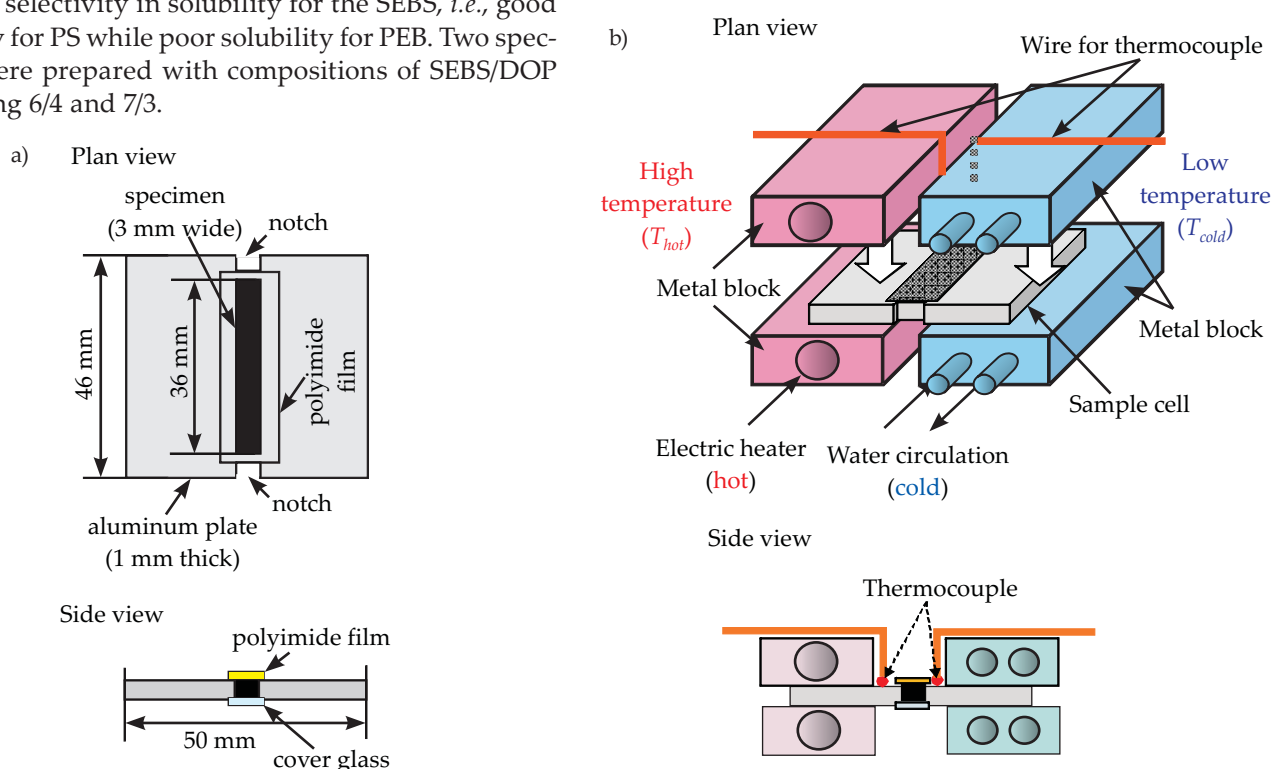

Fig. 1. Schematic illustrations for: a) the sample cell, b) fabrication of the set-up for imposing the temperature gradient

space to check their temperatures of both hot and cold sides. We have employed the same system before [17], but in this study we modified it to impose a larger extent of the temperature gradient.

The 2D-SAXS measurements for the specimens after the application of the temperature gradient were carried out at room temperature to analyze nanostructures and their orientation. The sample cell (the aluminum plate) was picked up from the set-up (shown in Fig. 1b) and was subjected to the 2D-SAXS measurements without removing the cover slip and the polyimide film. The 2D-SAXS measurements were conducted at the BL-6A beamline of the Photon Factory (High Energy Accelerator Research Organization, Tsukuba, Japan) [18], using X-ray with a wavelength of 0.150 nm. The sample to detector distance was 2.387 m and the beam size was measured at the detector position as 220 μm (a FWHM value) in the vertical direction and 560 μm (a FWHM value) in the horizontal direction. A PILATUS3-1M (DECTRIS Ltd., Baden, Switzerland) was used as a two-dimensional detector.

RESULTS AND DISCUSSION

Preliminary SAXS survey of the changes in nanostructures was carried out in the heating process at the heating rate of 10.7 °C/min for SEBS/DOP = 6/4 and 2.0 °C/min for SEBS/DOP = 7/3 with the time-resolved 2D-SAXS measurements in the interval of 30 s (each exposure times were 3 and 5 s for specimens with SEBS/DOP ratios of 6/4 and 7/3,

respectively). By conducting circular average of the resulted 2D-SAXS patterns, the 1D-SAXS profiles were obtained and the examples of the changes in the 1D-SAXS profiles as a function of temperature are shown in Fig. 2. Here, the scattering intensity is plotted against the magnitude of the scattering vector q in the semi-logarithmic manner. Value of q is defined as:

$$q = \frac{4\pi}{\lambda} \sin\frac{\theta}{2} \qquad (1)$$

where: λ, θ – the wavelength of X-ray and the scattering angle, respectively.

Note here that the profiles are shifted vertically to avoid overlaps. For both cases, two peaks are clearly observed with their peak positions (q values) relatively assigned to be 1:2 at the as-cast states. This fact indicates a lamellar morphology formed in both of the as-cast specimens. Considering that the volume fraction of PS is 0.16, the cylindrical morphology is preferred as the stable morphology for the case of bulk. Although the composition with 0.16 volume fraction of PS seems to be at the border between cylindrical and spherical phases, this composition can be considered to be in the stable cylindrical phase because of the strong segregation between PS and PEB chains. It can be also recognized that this composition is well in the stable cylindrical phase according to the theoretical phase diagram reported by Matsen and Bates [19]. From their phase diagram, the cylindrical phase can be considered as the stable state when $\chi \cdot N$ is larger than 43.6
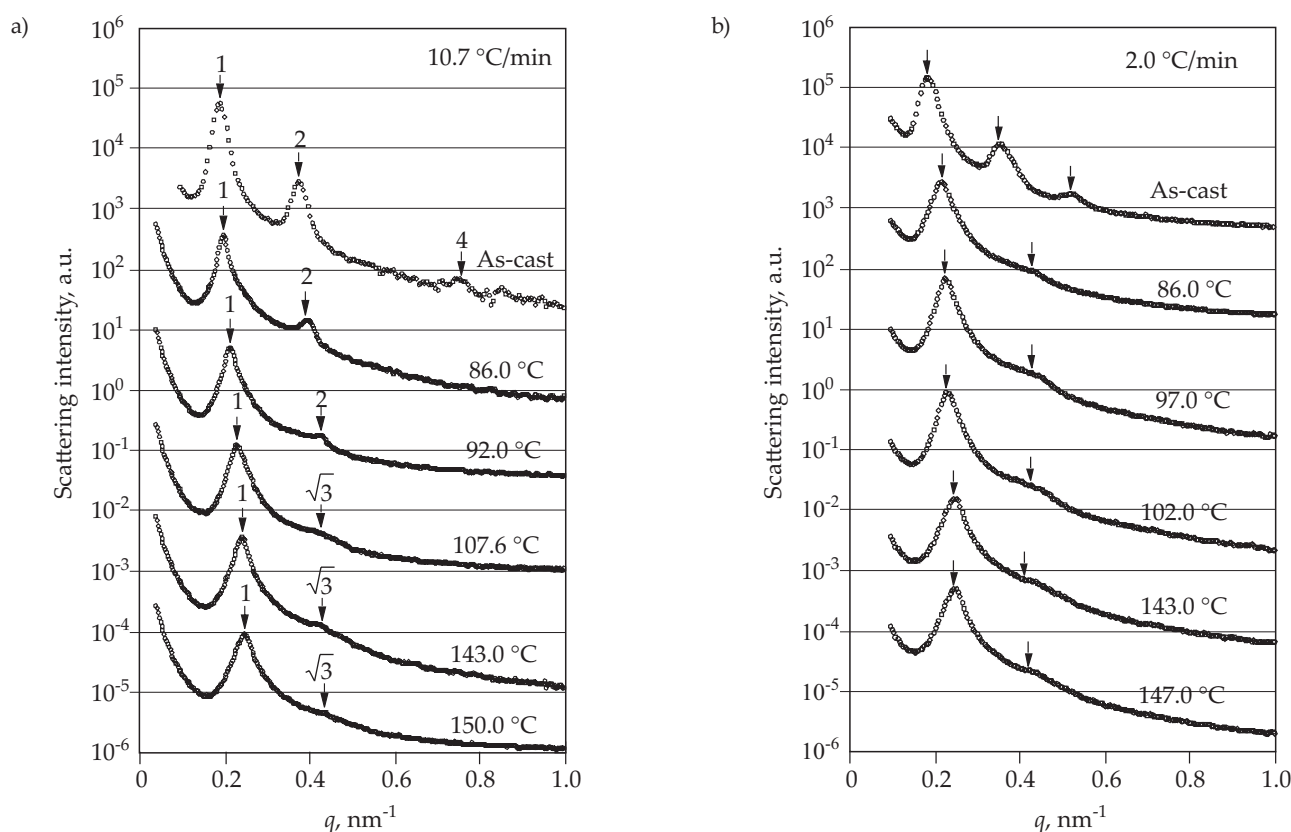

Fig. 2. Results of temperature scanning SAXS measurements in the heating process for specimens with: a) SEBS/DOP = 6/4, b) SEBS/DOP = 7/3

for $f = 0.16$ (χ, N and f denote the interaction parameter, the total degree of polymerization of the block copolymer and the volume fraction, respectively). The temperature dependence of the χ parameter has been reported in the literature [20] as $\chi = 0.0057 + 21/T$ (T denotes the absolute temperature). From the molecular weight value, $N = 1081$ is calculated. Thus, the range of the product of $\chi \cdot N$ is evaluated as $49.9 < \chi \cdot N < 82.3$ for the temperature range from room temperature to T_{ODT} (which is 246.5 °C for this particular sample). Since this range of $\chi \cdot N$ is above the border value of 43.6, the cylindrical phase is expected as the stable morphology for our particular sample (the SEBS triblock copolymer). As a matter of fact, the cylinder morphology has been confirmed as a stable state for the temperature range from room temperature to T_{ODT} in our previous studies [10]. Therefore, the reason of the formation of the lamellar structures is due to the selectivity in DOP solubility for SEBS. Namely, the DOP is preferred to exist in the PS microdomains, and therefore the effective volume fraction of the PS phase in the SEBS/DOP mixtures becomes higher than 0.16. As a matter of fact, it is seemed that the third-order peak disappeared in the profile of the specimen with SEBS/DOP ratio of 6/4 at the as-cast state, because the relative peak positions can be assigned as 1:2:4. The reason of the disappearance is due to the fact that the scattering function comprises lattice and particle factors. The former is interparticle interference owing to the regularity in packing of particles, while the latter is intraparticle interference due to a single particle. For the particular case of the lamellar system, the particle means a single lamella. Since the scattering function is in principle given by the product of those two factors, the third-order lattice peak disappears when the q-positions match for the third-order lattice peak and the destructive interference position of the particle scattering. Such condition is found to be simply governed by the volume fraction of PS being 0.333 [21]. This is surprising when considering that the PS fraction in the bulk is 0.16. From these values, we can evaluate the partition ratio ($x_{DOP/PS}$) of the DOP in the PS phase, which was 0.59 (for the as-cast state of the specimen with SEBS/DOP ratio of 6/4) supporting quantitatively that the DOP has selectivity to the PS phase. It is noted however that the third-order lattice peak does not disappear for the as-cast state of the specimen with SEBS/DOP ratio of 7/3. This is because the effective volume fraction of PS for this specimen is calculated as 0.29 by using $x_{DOP/PS} = 0.59$.

As temperature was elevated, the relative positions of the lattice peaks seemed to change both for the two specimens. To demonstrate clearly the change in the relative q-positions of the lattice peak, the relative ratio of the peak positions is plotted as a function of temperature in Fig. 3. It is then clearly observed that the value changed from 2 to $\sqrt{3}$ drastically at 99.8 °C for the specimen with SEBS/DOP = 6/4, while it changed gradually from 2 to $\sqrt{3}$ around 100.7 °C for the specimen with SEBS/DOP = 7/3.

The relative ratio of $\sqrt{3}$ suggests the hexagonal lattice of the cylindrical microdomains, which was also found
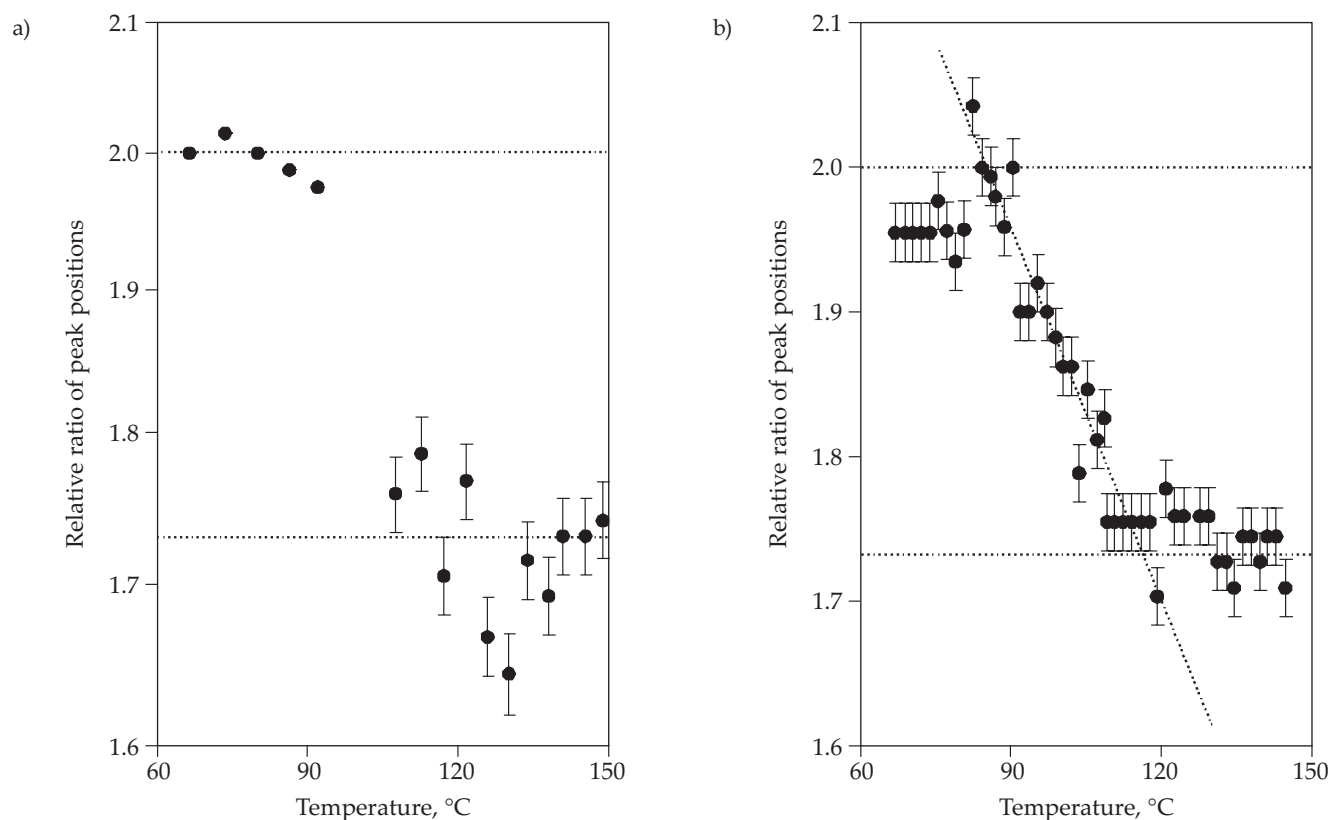

Fig. 3. Plot of the relative ratio of *q*-positions for the first- and second-order peaks as a function of temperature for specimens with: a) SEBS/DOP = 6/4, b) SEBS/DOP = 7/3

for the case of the bulk SEBS specimen [9–11]. Such order-order transition (OOT) is induced by the change in the partition of the DOP, implying that the value of $x_{DOP/PS}$ (the partition ratio of the DOP in the PS phase) may be decreased in some extent at higher temperature. It is surprising however that the OOT temperature (T_{OOT}) is almost the same for two specimens, irrespective of the compositions. We expected that T_{OOT} for the specimen with SEBS/DOP = 7/3 would be lower than that for the specimen with SEBS/DOP = 6/4, because the effective volume fraction is 0.29 for the case of first composition (SEBS/DOP = 7/3) assuming the same value of $x_{DOP/PS}$ as 0.59 at the as-cast state. This value of the effective volume fraction is very close to the border between lamellar and cylindrical morphologies in terms of A fraction in A-B-A triblock copolymers, and therefore the lamellar structure found in the as-cast specimen is expected to undergo OOT to cylinders when the partition of the DOP is slightly altered by elevating temperature. The gradual transition of the relative ratio of the peak position as shown in Fig. 3b implies that the formation of the cylinder microdomains would take place around 85.0 °C, which coexists with still remained lamellar microdomains below 116.5 °C. Thus, the temperature 85.0 °C for the onset of the cylinder formation is in good accord with the above-stated opinion that the T_{OOT} should be lower for the

Fig. 4. Plots of I_m^{-1} and σ_q^2 as a function of the inverse of the absolute temperature (T^{-1}) for the SEBS/DOP = 6/4 specimen (I_m and σ_q are the intensity and width of the first-order peak in the 1D-SAXS profile, respectively)

specimen with SEBS/DOP = 7/3 as compared to the case of SEBS/DOP = 6/4, although the average temperature for the former specimen is identical to T_{OOT} for the latter specimen. Such wide transition width of temperature for the specimen with SEBS/DOP = 7/3 may be due to a higher viscosity of PS/DOP phase, because the concentration of PS in the PS/DOP phase is higher for the composition with SEBS/DOP = 7/3 than for the composition with SEBS/DOP = 6/4. Actually, it was calculated as 0.39 and 0.29 for the former and the latter cases, respectively. Since the results shown in Fig. 3 were obtained in the heating process with constantly heating the specimens (2 °C/min), the equilibration of the structures (and therefore the OOT) cannot be attained in such a limited time range, although the glass transition temperature of the PS/DOP phase is much lower than room temperature even for these two specimens.

The plots of the inverse of the intensity and the square of the width (a FWHM value denotes as σ_q) for the first-order peak as a function of the inverse of the absolute temperature for the specimen with SEBS/DOP = 6/4, which is utilized for the determination of T_{ODT} are shown in Fig. 4. According to the criteria that the gaps in those plots indicate the occurrence of the order-disorder transition [22], it was evaluated T_{ODT} = 152.2 °C.

We now discuss the results of the control of orientation by imposing the temperature gradient to the SEBS/DOP = 6/4 specimen with 86 °C/143 °C for 3 h. Note that this condition meets $T_{cold} < T_{OOT} < T_{hot} < T_{ODT}$. Both temperatures, T_{cold} and T_{hot}, were directly increased from room temperature by taking special care to avoid overheating of the cold temperature above T_{OOT}. The resulted 2D-SAXS patterns as a function of the position of the specimen at which the incident X-ray beam (the beam size was 560 μm in the horizontal direction which is parallel to the temperature gradient direction) was irradiated are shown in Fig. 5. The normalized value of the integrated intensity for the first-order peak is shown together as a function of the azimuthal angle, which is defined as the angle counter-clock wise from the direction pointing the upward vertical. For the lower temperature side (a)–(c), almost circular pattern was observed. At 0.3 mm position (a), the peak intensity is almost constant, irrespective of the azimuthal angle. As the position is moved towards the higher temperature side, the peak intensity is likely accumulated in the equatorial direction in the order of (a) to (c). On the other hand, the hexagonal pattern was clearly observed for (d) to (f) positions, which is more clearly recognized in the plot of the azimuth-dependent intensity. Note here that the intense streaks appearing in the patterns of (e) and (f) is due to the X-ray beam hitting the edge of the sample cell (the higher temperature side). It is very striking that such hexagonal pattern was clearly observed at the higher temperature side, which indicates the significant orientation of cylinders perpendicular to the specimen surface. We will discuss such orientational state in details later.

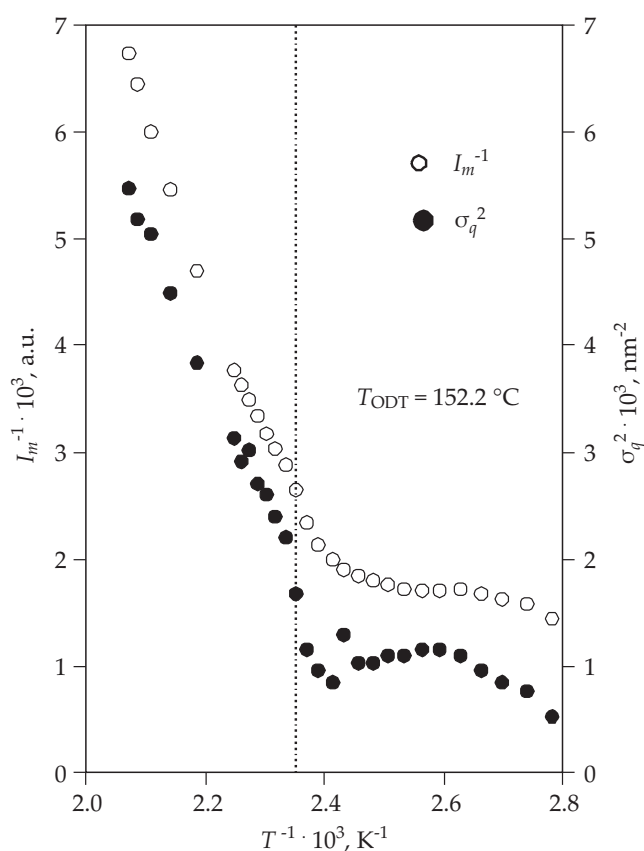To check rigorously the morphology corresponding to the 2D-SAXS patterns shown in Fig. 5, the sector average
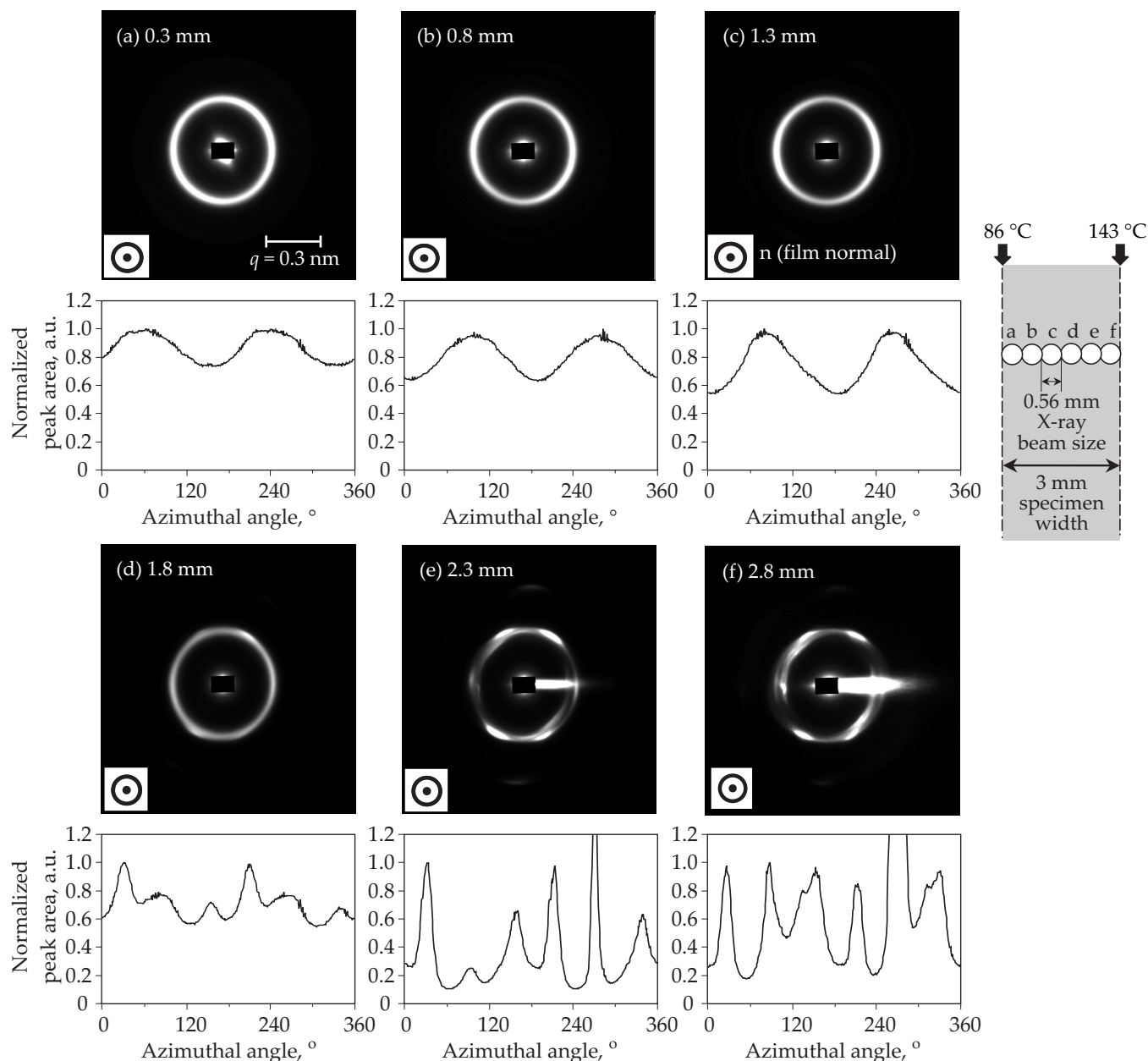
Fig. 5. Results of room temperature 2D-SAXS survey and azimuthal-angle dependence of the normalized integrated intensity (where the integrated intensity was normalized by its highest value) of the first-order peak for the SEBS/DOP = 6/4 specimen thermally annealed under the temperature gradient (86 °C/143 °C) by the scan of specimen positions parallel to the applied temperature gradient; (a) 0.3 mm, (b) 0.5 mm, (c) 1.0 mm, (d) 1.5 mm, (e) 2.0 mm, and (f) 2.5 mm from the cool temperature sidewall of the sample cell

of the pattern was conducted by using the area of the pattern with the azimuthal angle from 0° to 180° (namely the left half part of the 2D-SAXS pattern) to obtain 1D-SAXS profiles by avoiding the strong streak. The resulted 1D-SAXS profiles as a function of the specimen position are presented in Fig. 6. Again, it is very striking that the relative ratio of the peak positions can be assigned as $1{:}\sqrt{3}{:}\sqrt{7}$ for all of the profiles. As for the lower temperature side, the lamellar morphology should be expected because of $T_{cold} < T_{OOT}$. Therefore, it can be stated that the temperature gradient destabilized the lamellar structure. The disappearance of the $\sqrt{4}$ lattice peak for all of the 1D-SAXS profiles is very important upon consideration

of the reason why the lamellae were not formed. The condition of the disappearance of the $\sqrt{4}$ lattice peak for the cylindrical structure has been reported that the volume fraction of PS is 0.274 [23]. Value of $x_{DOP/PS}$ for this condition was calculated as 0.45, which indicates that the DOP is more or less evenly distributed in the SEBS and further implies that the DOP is no more selective diluent but a neutral diluent for the SEBS system. This preliminary conclusion is somewhat strange. Another possibility to explain the disappearance of the lamellar phase in the lower temperature side may be as follows. When the temperature gradient is applied to a fluid mixture with heavier and lighter components, the concentration gradi-
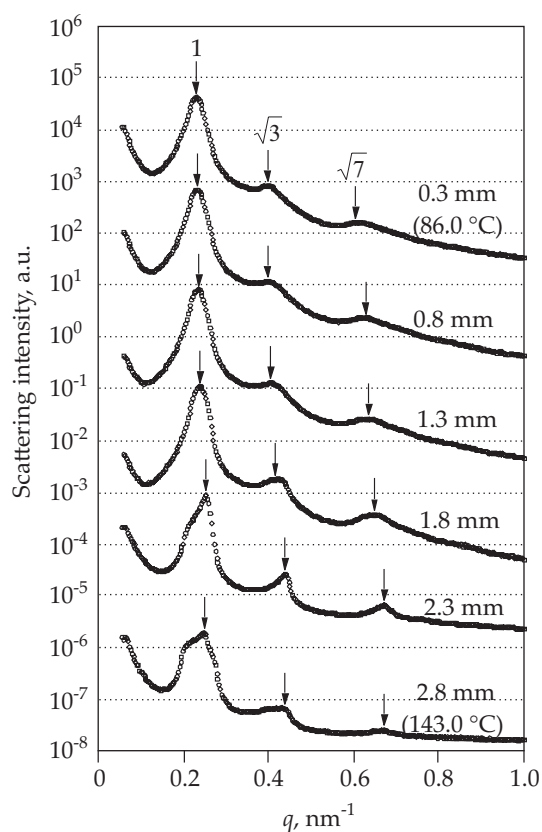
Fig. 6. 1D-SAXS profiles obtained from the 2D-SAXS patterns shown in Fig. 5 by conducting the sector average by using the area of the pattern with the azimuthal angle from 0° to 180° (namely the left half part of the 2D-SAXS pattern) to obtain 1D-SAXS profiles by avoiding the strong streak

Fig. 7. Schematic illustration of orientation of cylinders in the SEBS/DOP = 6/4 specimen thermally annealed under the temperature gradient (86 °C/143 °C)

ent is induced so as to accumulate the lighter component at the high temperature side. This phenomenon is known as the Ludwig-Soret effect [4]. If such effect is also applicable to our specimen, it can be considered that the DOP (which is the lighter component as compared to the SEBS triblock copolymer) content in the lower temperature side would be lower than 40 % (towards 30 % or lesser). As stated above, the lowering of the DOP content may decrease T_{OOT}, and as a matter of fact, the cylinder phase stably appeared around 86 °C for the case of composition with SEBS/DOP = 6/4. This would explain the appearance of the cylinder phase in the cold temperature side even for the case of the specimen with SEBS/DOP = 6/4 under the temperature gradient due to the Ludwig-Soret effect.

We then discuss the details of the orientational state in the specimen. Schematic illustration of the orientation of cylinders in the specimen thermally annealed under the temperature gradient with 86 °C/143 °C for 3 h is shown in Fig. 7. As stated above, closer to the cold temperature side, the overall orientation is random, while the cylinders are perpendicularly oriented near the high temperature side. Furthermore, the result of the hexagonal spots in the 2D-SAXS pattern shown in Fig. 5f (even scattering intensity with almost 60° azimuthal angle repeat of six peaks) indicates an orientation where (10$\bar{1}$0) planes
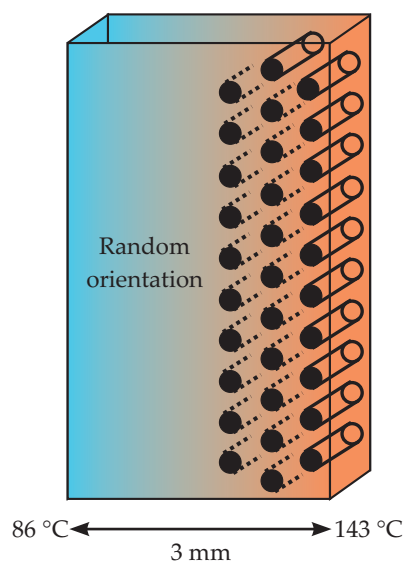
of the hexagonal lattice are parallel to the surface of the hot temperature wall of the sample holder, as shown in Fig. 7. Note here that such an orientational state is stable because maximum numbers of cylinders are placed on the (10$\bar{1}$0) planes. Furthermore, since both of the spacing and the cylinder radius becomes larger as the temperature is decreased (the spacing ~ $T^{1/3}$) [24, 25], such an orientational state is considered to accommodate well the cylinders in the confined space under the temperature gradient. Namely, in case when the cylinders would be formed parallel to the direction of the temperature gradient, the radius of the cylinders should be increasing in the cylinder axis direction. It should be noted here that the same condition should be met at the same time for the spacing (in other words, the distance between neighboring cylinders should also increase). It is impossible to meet these requirements together for the case of the orientation of the cylinders parallel to the temperature gradient direction.

Then, how about considering another extreme case of the orientation where the cylinders are parallel both to the specimen surface and to the surface of the sidewall of the sample cell? The above stated requirements (the spacing and the cylinder radius should increase with the decrease in temperature) can be met without difficulty in this case. Thus, this orientational state would take place equally with the perpendicular orientation as observed in our experimental study. However, the result of the even distribution of the scattering intensity for the 6 spots of the first-order peaks as a function of the azimuthal angle (as shown in Fig. 5f) excludes the additional existence of such an orientational state which would increase the intensity in the equatorial direction (at the azimuthal angles of 90° and 270°). Considering the size of the specimen space in the sample holder of 3 mm in the temperature gradient direction while it is quite long as 36 mm in the direction parallel to the sidewall (see Fig. 1), very long cylinders are requested to be formed

in case of the orientational state with cylinders parallel to the sidewall. As contrast, the requested length of cylinders is as short as 1 mm (which is the thickness of the sample cell) in the case of the perpendicular orientation that we experimentally found in this study. The latter requirement is much easier to meet as compared to the former case. This may be a reason why the perpendicular orientation of cylinders as schematically shown in Fig. 7 was obtained. To make sure of the orientational state, we recognize our experimental results of the through-view measurements are not satisfactory and the other views such as edge- and end-views are at least required.

CONCLUSIONS

We examined the significance of the effect of the temperature gradient for the control of the orientation of the microdomains. For this purpose, the tremendous extent of temperature difference (T_{cold} - T_{hot} = 143 °C - 86 °C = 57 °C) was successfully imposed to the SEBS/DOP = 6/4 specimen with 3 mm width (the gradient is as high as 19.0 K/mm). The 2D-SAXS measurements revealed that the cylindrical morphology was found near the cold sidewall of the sample cell, even though the cold temperature was below T_{OOT} and therefore the lamellar phase should be stable. This result implies that the temperature gradient may destabilize the lamellar phase. More interestingly, perpendicularly oriented cylinders (the cylinder axes are perpendicular to the sheet specimen) were formed near the hot sidewall of the sample cell with the orientation that the ($10\bar{1}0$) planes of the hexagonal lattice are parallel to the surface of the hot temperature sidewall of the sample cell. Since both of the spacing and the cylinder radius become larger as the temperature is decreased, such an orientational state is considered to accommodate well the cylinders in the confined space under the temperature gradient.

REFERENCES

[1] Singh G., Yager K.G., Smilgies D.-M. *et al.*: *Macromolecules* **2012**, *45*, 7107.
http://dx.doi.org/10.1021/ma301004j

[2] Xue J., Singh G., Qiang Z. *et al.*: *Nanoscale* **2013**, *5*, 7928. http://dx.doi.org/10.1039/C3NR02821F

[3] Deguchi M., Kimura G., Shimizu N. *et al.*: *Journal of the Society of Materials Science Japan* **2017**, *66*, 7.
http://dx.doi.org/10.2472/jsms.66.7

[4] de Groot S.R., Mazur P.: "Nonequilibrium Thermodynamics", Dover, New York 1984.

[5] Sakurai S., Wang Y.-C., Kushiro T.: *Chemical Physics Letters* **2001**, *348*, 242.
http://dx.doi.org/10.1016/S0009-2614(01)01102-2

[6] Nambu T., Yamauchi Y., Kushiro T., Sakurai S.: *Faraday Discussions* **2005**, *128*, 285.
http://dx.doi.org/10.1039/B403108C

[7] Hashimoto T., Bodycomb J., Funaki Y., Kimishima K.: *Macromolecules* **1999**, *32*, 952.
http://dx.doi.org/10.1021/ma9815410

[8] Bodycomb J., Funaki Y., Kimishima K., Hashimoto T.: *Macromolecules* **1999**, *32*, 2075.
http://dx.doi.org/10.1021/ma981538g

[9] Sakurai S.: *Polymer* **2008**, *49*, 2781.
http://dx.doi.org/10.1016/j.polymer.2008.03.020

[10] Sakurai S., Bando H., Yoshida H. *et al.*: *Macromolecules* **2009**, *42*, 2115.
http://dx.doi.org/10.1021/ma900155n

[11] Ohnogi H., Isshiki T., Sasaki S., Sakurai S.: *Nanoscale* **2014**, *6*, 10 817.
http://dx.doi.org/10.1039/C4NR02074J

[12] Asaoka S., Uekusa T., Tokimori H. *et al.*: *Macromolecules* **2011**, *44*, 7645.
http://dx.doi.org/10.1021/ma201119u

[13] Cui G., Ohya S., Matsutani T. *et al.*: *Nanoscale* **2013**, *5*, 6713. http://dx.doi.org/10.1039/C3NR01491F

[14] Cui G., Fujikawa M., Nagano S. *et al.*: *Polymer* **2014**, *55*, 1601. http://dx.doi.org/10.1016/j.polymer.2014.01.060

[15] Komura M., Yoshitake A., Komiyama H., Iyoda T.: *Macromolecules* **2015**, *48*, 672.
http://dx.doi.org/10.1021/ma501874z

[16] Folkes M.J., Keller A.: *Polymer* **1971**, *12*, 222.
http://dx.doi.org/10.1016/0032-3861(70)90067-4

[17] Yasuda A., Yamane M., Yamanishi H. *et al.*: *Journal of the Society of Materials Science Japan* **2011**, *60*, 57.

[18] Shimizu N., Mori T., Igarashi N. *et al.*: *Journal of Physics: Conference Series* **2013**, *425*, 202 008.

[19] Matsen M.W., Bates F.S.: *Macromolecules* **1996**, *29*, 1091. http://dx.doi.org/10.1021/ma951138i

[20] Owens J.N., Gancarz I.S., Koberstein J.T., Russell T.P.: *Macromolecules* **1989**, *22*, 3380.
http://dx.doi.org/10.1021/ma00198a032

[21] Matsushita Y., Momose H., Yoshida Y., Noda I.: *Polymer* **1997**, *38*, 149.

[22] Sakamoto N., Hashimoto T., Kido R., Adachi K.: *Macromolecules* **1996**, *29*, 8126.
http://dx.doi.org/10.1021/ma9609487

[23] Sakurai S., Umeda H., Furukawa C. *et al.*: *The Journal of Chemical Physics* **1998**, *108*, 4333.
http://dx.doi.org/10.1063/1.475834

[24] Shibayama M., Hashimoto T., Kawai H.: *Macromolecules* **1983**, *16*, 16.
http://dx.doi.org/10.1021/ma00235a005

[25] Hashimoto T., Shibayama M., Kawai H.: *Macromolecules* **1983**, *16*, 1093.
http://dx.doi.org/10.1021/ma.00241a010